Global temperature calibration of the alkenone unsaturation index ($U_{37}^{K'}$) in surface waters and comparison with surface sediments

Maureen H. Conte
Department of Marine Chemistry and Geochemistry, Woods Hole Oceanographic Institution, Woods Hole, Massachusetts 02543, USA (mconte@bbsr.edu)

Now at Bermuda Biological Station for Research, Inc., Ferry Reach, St. Georges GE01, Bermuda

Marie-Alexandrine Sicre
Laboratoire des Science du Climat et de l'Environnement, CNRS SDU UMR 1572, Domaine du CNRS, Ave de la Terrasse, F-91191 Gif-sur-Yvette Cedex, France

Carsten Rühlemann
Bundesanstalt für Geowissenschaften und Rohstoffe, Referat B3.23, Meeresgeologie und Tiefseebergbau, Stilleweg 2, D-30655 Hannover, Germany

Also at DFG Forschungszentrum Ozeanränder der Universität Bremen, Leobener Str., D-28359 Bremen, Germany

John C. Weber
Department of Marine Chemistry and Geochemistry, Woods Hole Oceanographic Institution, Woods Hole, Massachusetts 02543, USA

Now at The Ecosystems Center, Marine Biological Laboratory, Woods Hole, Massachusetts 02543

Sonja Schulte
Institut für Chemie und Biologie des Meeres, Carl von Ossietzky Universität Oldenburg, Carl-von-Ossietzky-Str. 9-11, D-26111 Oldenburg, Germany

Detlef Schulz-Bull
Department of Marine Chemistry, Institute for Baltic Sea Research-Warnemünde, University of Rostock, Seestrasse 15, D-18119 Rostok-Warnemuende, Germany

Thomas Blanz
Department of Marine Chemistry, Institute for Baltic Sea Research-Warnemünde, University of Rostock, Seestrasse 15, D-18119 Rostok-Warnemuende, Germany

Now at Institut für Geowissenschaften der Christian Albrechts Universität Kiel, Ludewig-Meyn-Str. 10, D-24118 Kiel, Germany

[1] In this paper, we compile the current surface seawater C_{37} alkenone unsaturation ($U_{37}^{K'}$) measurements (n = 629, −1 to 30°C temperature range) to derive a global, field-based calibration of $U_{37}^{K'}$ with alkenone production temperature. A single nonlinear "global" surface water calibration of $U_{37}^{K'}$ accurately predicts alkenone production temperatures over the diversity of modern-day oceanic environments and alkenone-synthesizing populations (T = −0.957 + 54.293($U_{37}^{K'}$) − 52.894($U_{37}^{K'}$)^2 + 28.321($U_{37}^{K'}$)^3, r^2 = 0.97, n = 567). The mean standard error of estimation is 1.2°C with insignificant bias in estimated production temperature among the different ocean regions sampled. An exception to these trends is regions characterized by strong lateral advection and extreme productivity and temperature gradients (e.g., the Brazil-Malvinas Confluence). In contrast to the surface water data, the calibration of $U_{37}^{K'}$ in surface sediments with

overlying annual mean sea surface temperature (AnnO) is best fit by a linear model (AnnO = $29.876(U_{37}^{K'}) - 1.334$, $r^2 = 0.97$, n = 592). The standard error of estimation (1.1°C) is similar to that of the surface water production calibration, but a higher degree of bias is observed among the regional data sets. The sediment calibration differs significantly from the surface water calibration. $U_{37}^{K'}$ in surface sediments is consistently higher than that predicted from AnnO and the surface water production temperature calibration, and the magnitude of the offset increases as the surface water AnnO decreases. We apply the global production temperature calibration to the coretop $U_{37}^{K'}$ data to estimate the coretop alkenone integrated production temperature (coretop IPT) and compare this with the overlying annual mean sea surface temperature (AnnO). We use simple models to explore the possible causes of the deviation observed between the coretop temperature signal, as estimated by $U_{37}^{K'}$, and AnnO. Our results indicate that the deviation can best be explained if seasonality in production and/or thermocline production as well as differential degradation of 37:3 and 37:2 alkenones both affect the sedimentary alkenone signal.

1. Introduction

[2] The use of C_{37} alkenone unsaturation ($U_{37}^{K'}$) to estimate sea surface temperature is now firmly established as a valuable paleoceanographic tool. $U_{37}^{K'}$ is defined as

$$U_{37}^{K'} = \frac{C37:2}{(C37:3 + C37:2)}, \quad (1)$$

where C37:2 and C37:3 are the concentrations of the di- and tri- unsaturated C_{37} alkenones, respectively. The ubiquitous presence of alkenones throughout the world's oceans [*Marlowe et al.*, 1990], the robustness of the alkenone temperature signal in sediments (reviewed by *Grimalt et al.* [2000]), and their persistence throughout the stratigraphic record [*Marlowe et al.*, 1990] make alkenones uniquely valuable for a variety of investigations over a range of timescales.

[3] Since the initial discovery of $C_{37}-C_{39}$ alkenones in sediments [*Boon et al.*, 1978] and their origins in the haptophyte algae *Emiliania huxleyi* and related species [*Volkman et al.*, 1980; *Marlowe*, 1984], a wide range of alkenone studies both in culture [*Marlowe*, 1984; *Prahl et al.*, 1988; *Volkman et al.*, 1995; *Sawada et al.*, 1996; *Conte et al.*, 1998; *Epstein et al.*, 1998; *Yamamoto et al.*, 2000] and in surface waters [*Prahl and Wakeham*, 1987; *Conte et al.*, 1992, 1994, 2001; *Conte and*

Eglinton, 1993; *Ternois et al.*, 1997; *Sicre et al.*, 2002] have demonstrated the close linkage between alkenone unsaturation ratios and growth temperature. In addition to growth temperature, it is also clear that alkenone unsaturation is influenced by genetic and physiological factors [*Conte et al.*, 1994, 1995, 1998; *Sawada et al.*, 1996; *Epstein et al.*, 1998; *Yamamoto et al.*, 2000], but the extent that these factors bias paleo temperature estimates is unresolved. Uncertainties also exist in the environmental interpretation of the alkenone temperature signal in sediments (reviewed by *Volkman* [2000] and *Bijma et al.* [2001]). Does seasonality in alkenone production or inputs from thermocline synthesis of alkenones bias the alkenone temperature signal in sediments? Do diagenetic processes and/or fine particle advection create discrepancies between the alkenone signal in the sediments from that of overlying production?

[4] To provide insight into these questions, we have compiled 1400 data on alkenone distributions in the surface mixed layer and underlying surface sediments. These data were collected from throughout the world's oceans. We calibrate $U_{37}^{K'}$ in surface waters against growth temperature for each ocean region and for the combined "global" surface water data. We next use this surface water production temperature calibration to calculate the "integrated production temperature (IPT)" that is

Table 1. Alkenone Surface Water (0–30 m) Data Sources[a]

Geographic Area	n	Data Sources
Atlantic region	*451*	
Nordic Sea	39	*Sicre et al.* [2002]; *Bendle and Rosell-Melé* [2004]
North Atlantic	124	*Brassell et al.* [1986]; *Conte et al.* [1992]; *Conte and Eglinton* [1993]; *Sicre et al.* [2002]; *Bendle and Rosell-Melé* [2004]; M. Conte and J. C. Weber (unpublished data); D. Shultz-Bull and T. Blanz (unpublished data); C. Rühlemann and S. Schulte (unpublished data)
Bermuda	88	*Conte et al.* [2001]
Tropical Atlantic (10°N–10°S)	35	M. Conte and J. C. Weber (unpublished data); C. Rühlemann et al. (unpublished data)
NE Atlantic upwelling	6	M. Conte and J. C. Weber (unpublished data)
Caribbean	20	C. Rühlemann and S. Schulte (unpublished data); *Prahl and Wakeham* [1987]
South Atlantic	40	C. Rühlemann et al. (unpublished data)
Argentine Basin	59	C. Rühlemann et al. (unpublished data)
Norwegian fjords	14	*Conte et al.* [1994]
Mediterranean Sea	26	*Ternois et al.* [1997]; *Bentaleb et al.* [1999]; *Cacho et al.* [1999]
Pacific region	*131*	
NE Pacific	32	*Prahl and Wakeham* [1987], *Prahl et al.* [2003], *Bac et al.* [2003], F. Prahl (unpublished data)
Equatorial Pacific	12	M.-A. Sicre (unpublished data)
Hawaii[b]	5	*Prahl et al.* [2005]
Western Pacific	68	*Sawada et al.* [1998]; *Hamanaka et al.* [2000]; *Bentaleb et al.* [2002]
W. Pacific, *G. oceanica* bloom	1	N. Ohkouchi (unpublished data)
Bering Sea	12	*Shin et al.* [2002]; *Harada et al.* [2003]
Peru Upwelling	1	*Prahl and Wakeham* [1987]
Indian Ocean region	*5*	
Arabian Sea	3	M.-A. Sicre (unpublished data)
S. Indian Ocean	2	M.-A. Sicre (unpublished data)
Southern Ocean	*42*	
Southern Ocean	41	*Sikes and Volkman* [1993]
Southern Ocean[c]	1	A. Benthien (unpublished data)
Total surface water data	*629*	

[a] The sample locations are shown in Figure 1.
[b] Each data point is the mean of 5–8 replicated measurements.
[c] Samples were collected within an Fe enriched water mass; data is mean of 16 measurements.

recorded by $U^{K'}_{37}$ in the sediments. This analysis shows that the coretop alkenone production temperature ("coretop IPT") is systematically offset from overlying annual mean sea surface temperature (AnnO), as estimated by the Levitus 2001 updated compilation of ocean temperatures [*Conkright et al.*, 2002]. We examine possible explanations for this offset.

2. Data Sources

[5] The 629 surface mixed layer (0–30 m) alkenone data we compile (Table 1) include nearly 200 unpublished data as well as data from previously published studies. The locations of these surface water samples are plotted in Figure 1. We include in this data set only alkenone data from samples collected within the surface mixed layer and exclude any samples collected from within the seasonal thermocline to eliminate any possibility of confounding effects from the presence of detrital alkenones synthesized in the warmer, overlying mixed layer [cf. *Sicre et al.*, 2002]. The surface water data sets include both samples collected along transects in a single season as well as repeated measurements at fixed station locations
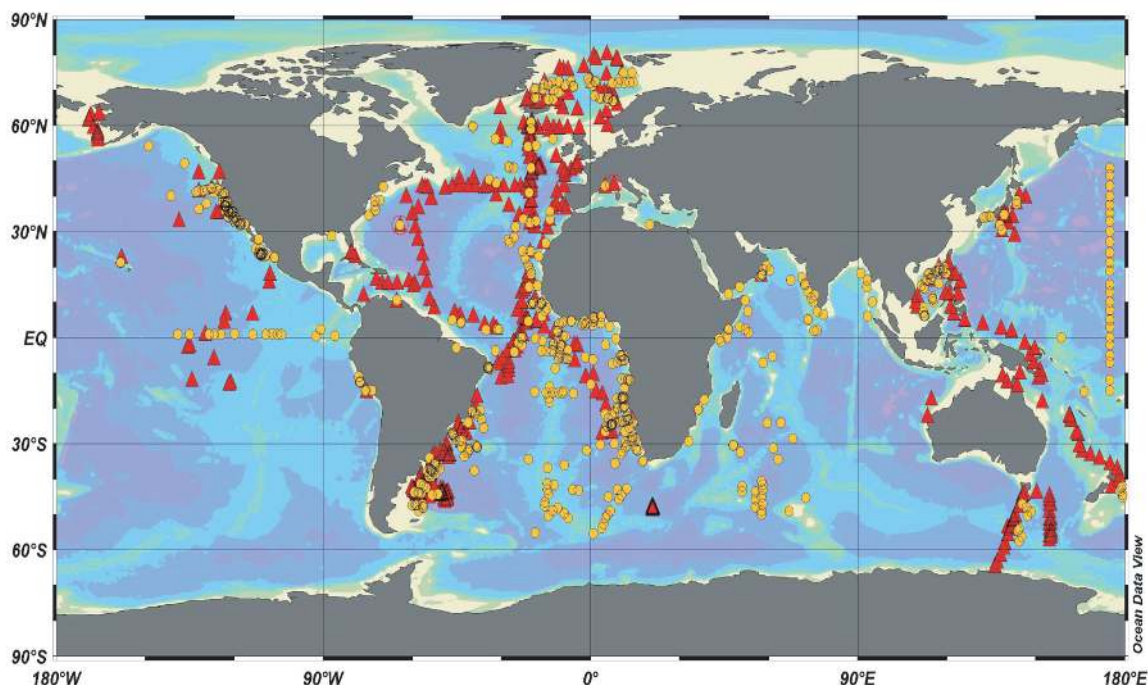
Figure 1. Map of sample locations of surface water (red solid triangles) and coretop sediment (yellow solid circles) data. Locations of time series sites where surface waters were sampled over the seasonal cycle are circled. References for the surface water and sediment data are given in Tables 1 and 2, respectively. Map produced using Ocean Data View (R. Schlitzer, 2004; available at http://www.awi-bremerhaven.de/GEO/ODV).

over the seasonal temperature cycle (e.g., the Bermuda BATS/OFP and Mediterranean DYFAMED time series). The surface water data set is heavily weighted toward samples from the Atlantic region, which comprise 71% of the total. The Pacific region comprises 21% of the data, with the majority of the samples collected near continental margins. Data from the Southern Ocean comprises 7% of the total, with 60% of the samples collected north of the Antarctic polar front. The Indian Ocean region is very sparsely sampled, with only five data.

[6] To compare the surface and sediment distributions, we have also compiled 742 surface sediment ("coretop") data from unpublished and published sources (Table 2). The locations of the sediment samples are also mapped in Figure 1. It is obvious from this map that deep ocean sediments of the central gyres are very poorly sampled relative to the continental margins. The sediment data are heavily weighted toward the South Atlantic and NE Pacific margin sediments, which comprise 31% and 12% of the samples, respectively. There is good geographical overlap between the surface water and sediment samples in the eastern Atlantic, the Mediterranean, the western South Atlantic and

North Pacific margins and in the Southern Ocean south of Tasmania. In other regions, there is minimal geographic overlap.

[7] For the surface mixed layer temperatures, we have used the water temperature measured at the time of sample collection. This was measured either using temperature probes on CTD casts taken at or near the time of sample collection or from temperature probes mounted on flow-through water collection systems. For the surface sediment data, we have estimated the annual mean temperature of the overlying surface mixed layer at 0 m depth (AnnO) for the sediment sample location using the updated Levitus 2001 compilation [*Conkright et al.*, 2002]. For some sediment data, the updated Levitus temperatures are up to 1–2°C different from the temperatures that were reported in the original papers.

3. Statistical Analyses

[8] Linear and polynomial regressions were computed using standard regression techniques. MATLAB (Mathworks, Natick MA) and SYSTAT statistical packages were used for computations.

Table 2. Alkenone Coretop Sediment Data Sources[a]

Geographic Area	n	References
Atlantic region	*436*	
Nordic Sea	47	*Rosell-Melé et al.* [1995]; *Rosell-Melé* [1998]
North Atlantic	44	*Sikes et al.* [1991]; *Madureira* [1994]; *Sikes and Keigwin* [1994]; *Rosell-Melé et al.* [1995]; *Chapman et al.* [1996]; *Müller and Fischer* [2001, 2003]; T. Herbert (unpublished data)
Northwest Atlantic	7	*Sikes et al.* [1991]; T. Herbert (unpublished data)
Caribbean/Gulf of Mexico	8	T. Herbert (unpublished data)
Equatorial Atlantic (10°S to 10°N)	102	*Sikes et al.* [1991]; *Madureira* [1994]; *Sikes and Keigwin* [1994]; *Rosell-Melé et al.* [1995]; *Müller et al.* [1998]; *Benthien and Müller* [2000]; T. Herbert (unpublished data)
South Atlantic	135	*Müller et al.* [1998]; *Benthien and Müller* [2000]; *Müller and Fischer* [2003]
Southwest Atlantic margin	96	*Benthien and Müller* [2000]
Mediterranean	4	*Cacho et al.* [1999]
Pacific region	*209*	
Peru/Chilean Upwelling	14	*McCaffrey et al.* [1990], *Sikes et al.* [1991]; *Kim et al.* [2002]; T. Herbert (unpublished data)
Subtropical/Equatorial Pacific	31	*Prahl et al.* [1989]; T. Herbert (unpublished data)
NE Pacific	12	*Sikes et al.* [1991]; *Doose et al.* [1997]
California Margin/NE Pacific margin	86	*Kennedy and Brassell* [1992]; *Doose et al.* [1997]; *Herbert et al.* [1998]; *Goñi et al.* [2001]; T. Herbert (unpublished data)
Hawaii	2	T. Herbert (unpublished data)
Central North Pacific, 175°E transect	20	*Ohkouchi et al.* [1999]
NW Pacific/Japan Sea	9	*Sawada et al.* [1996]
South China Sea	31	*Pelejero and Grimalt* [1997]
Indian Ocean region	*78*	
South Indian Ocean	23	*Sikes et al.* [1997]
Indian Ocean/Arabian Sea	55	*Sonzogni et al.* [1997]; *Budziak* [2001]; T. Herbert (unpublished data)
Southern Ocean	*19*	*Sikes et al.* [1997]; *Ikehara et al.* [1997]
Total surface sediment data	*742*	

[a] The sample locations are shown in Figure 1.

The calibration models were computed in three steps. An initial regression of all data was performed to identify outliers (>3x the standard deviation) which were then removed from the data set. Next, we computed a 3rd order polynomial regression and checked whether the higher order terms were significant. If so, they were retained in the calibration model. We again checked for outliers and also eliminated data with excessive leverage [*Neter and Wasserman*, 1974] from the final calibration data set, as these would have undue influence on the final calibration model and increase estimation error.

[9] To evaluate the difference between the surface water and coretop $U^{K'}_{37}$ calibrations we used a standard parametric test for equivalence of two regression lines, as described in detail by *Neter and Wasserman* [1974] and similar statistical texts.

4. Results

4.1. Relationship Between Alkenone $U^{K'}_{37}$ and Temperature in Surface Waters

[10] The $U^{K'}_{37}$ in surface mixed layer particles versus measured water temperature is plotted in Figure 2 for the ocean basins individually and for the combined global data set. The samples from the Atlantic and adjacent regions (Figure 2a) range over −1 to 29°C. The different regions have very similar $U^{K'}_{37}$ versus temperature relationships, as seen by the agreement in the plotted data. This
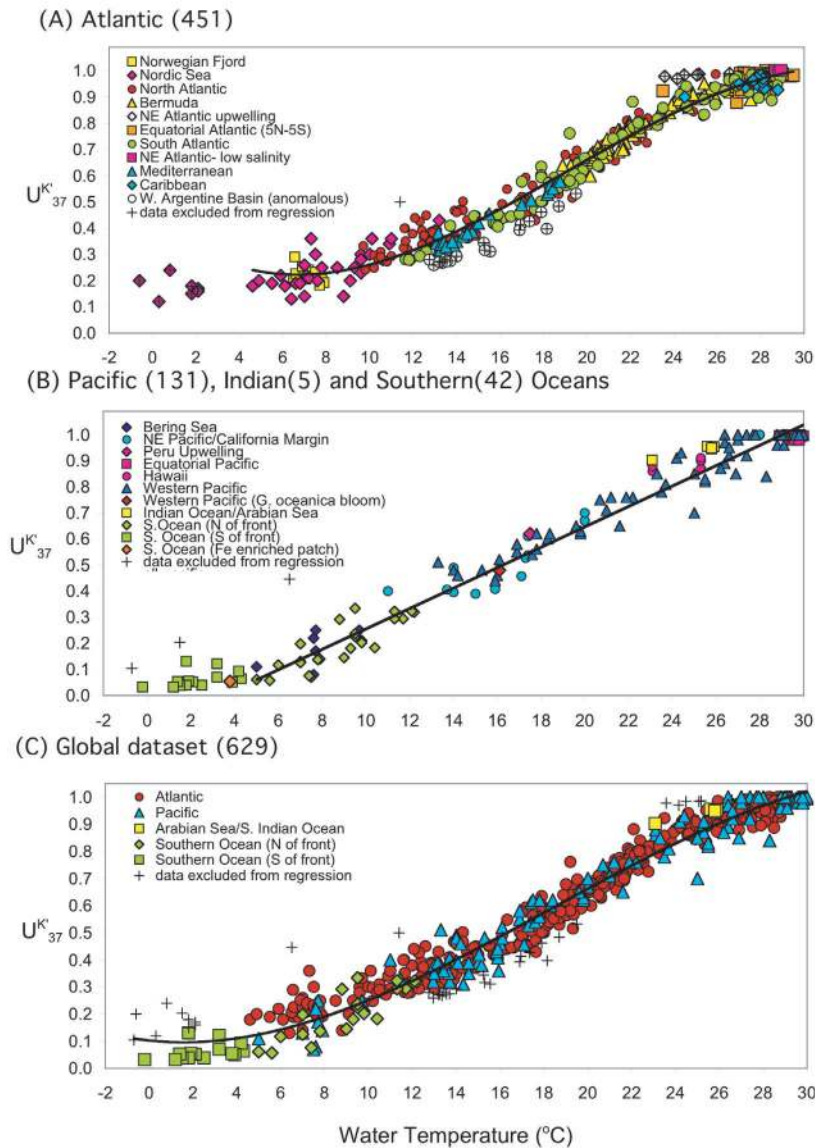
Figure 2. $U_{37}^{K'}$ versus measured water temperature for surface mixed layer (0–30 m) samples. (a) Atlantic region. The empirical 3rd order polynomial regression for samples collected in >4°C waters, excluding outlier data from the southwest Atlantic margin and northeast Atlantic upwelling regime, is $U_{37}^{K'} = -1.004 \times 10^{-4}T^3 + 5.744 \times 10^{-3}T^2 - 6.207 \times 10^{-2}T + 0.407$ ($r^2 = 0.98$, $n = 413$). (b) Pacific, Indian, and Southern Ocean regions. The empirical linear regression of Pacific samples is $U_{37}^{K'} = 0.0391T - 0.1364$ ($r^2 = 0.97$, $n = 131$). Please note the Pacific regression does not include the Indian and Southern Ocean data. (c) Global data. The empirical 3rd order polynomial regression, excluding anomalous southwest Atlantic margin data, is $U_{37}^{K'} = -5.256 \times 10^{-5}T^3 + 2.884 \times 10^{-3}T^2 - 8.4933 \times 10^{-3}T + 9.898$ ($r^2 = 0.97$, $n = 588$). Samples that were excluded from the regressions are shown by crosses.

agreement is striking given the fact that the different sample sets were collected in different seasons and across productivities ranging from oligotrophy to *E. huxleyi* blooms. For example, strong agreement is observed among Mediterranean and Bermuda time series data, eastern North Atlantic data collected along a 20°W transect in spring/summer and North Atlantic data collected along an east-west mid latitude transect in late summer/fall. In

warmer waters, strong agreement is observed between samples collected off Bermuda, which are dominated by *E. huxleyi* throughout the year [*Haidar and Thierstein*, 2001] and equatorial Atlantic samples in which *G. oceanica* and *E. huxleyi* are co-dominant (M. Conte and P. Ziveri, personal observations). The equatorial Atlantic samples also include samples that were collected from within a low salinity water mass; the agree-

ment indicates that salinity influences on $U_{37}^{K'}$ in the open ocean are minimal. In cold water regions, good agreement is observed between samples from Norwegian fjords, where *E. huxleyi* populations contain high concentrations of tetraunsaturated alkenones [*Conte et al.*, 1994] and samples from the high latitude North Atlantic [*Sicre et al.*, 2002] and Iceland Basin [*Conte and Eglinton*, 1993], where populations contain high concentrations of alkyl alkenoates but low concentrations of tetraunsaturated alkenones relative to the Norwegina fjord populations. This general agreement occurs despite the poor correlations that have been observed between $U_{37}^{K'}$ and growth temperature across more limited temperature ranges within each basin (e.g., in the Norwegian Fjord and Iceland Basin). The consistency in the alkenone versus growth temperature relationship across these diverse settings demonstrates that growth temperature exerts the major control on the $U_{37}^{K'}$ in oceanic settings.

[11] Two data sets show a significant deviation from the Atlantic trend line. The first is composed of samples from the western Argentine Basin which, as discussed in the following section, appear to have been influenced by lateral advection. The second is a small group of samples collected near the upwelling region off Cape Verde. The temperatures of these samples are several degrees cooler than predicted by their $U_{37}^{K'}$ ratios. The reason for this offset is not clear, as samples collected previously in this area [*Conte and Eglinton*, 1993] did not deviate from the general trend.

[12] Nonlinearity in the relationship between $U_{37}^{K'}$ with growth temperature is also clearly present in the Atlantic data. This nonlinear relationship is adequately approximated by an empirical third order polynomial regression. Nonlinearity has been previously observed in cultured algae [*Conte et al.*, 1998] as well as at Bermuda over the annual cycle [*Conte et al.*, 2001]. The reduction in slope at the temperature extremes (i.e., for water temperatures <5°C or >26°C) evidences the weaker temperature dependence of $U_{37}^{K'}$ at the limits of the growth temperature range of *E. huxleyi*. This scatter reflects both a greater influence of non-temperature related factors on alkenone unsaturation near the limits of the temperature response [e.g., *Conte et al.*, 1998], and also the greater measurement error as the $U_{37}^{K'}$ function approaches its asymptotes [*Grimalt et al.*, 2000; *Pelejero and Calvo*, 2003]. In addition, part of this scatter and reduction in slope of $U_{37}^{K'}$ at the cold water end may reflect the role of tetraunsaturated alkenones in the physiological response. There is also somewhat higher

scatter in the data, especially that of cold water regions.

[13] Data from the Pacific, Indian and Southern Oceans are plotted in Figure 2b. The data sets from these regions also exhibit a remarkable degree of agreement considering the diversity of environments sampled. Significantly, there is excellent agreement between samples in which *Gephyrocapsa* spp. is the major alkenone synthesizer (e.g., in the western Pacific) and samples from regions where *E. huxleyi* is the major alkenone synthesizer. The agreement clearly does not support the suggestion [*Volkman et al.*, 1995; *Sawada et al.*, 1996] that *Gephyrocapsa* spp. are different from *E. huxleyi* in regards to their alkenone versus growth temperature relationship. As in the Atlantic, the incremental change in $U_{37}^{K'}$ per °C becomes nonsignificant at low temperatures, as observed for samples collected in <6°C waters south of the Antarctic front. A polynomial regression was similarly computed for the Pacific data. The higher order terms in the regression were not significant for the Pacific dataset, so a linear regression was fit. This regression is similar to that reported by *Prahl and Wakeham* [1987] for a subset of these data.

[14] In Figure 2c, we plot the entire global surface water data to underscore the striking agreement in the dependence of $U_{37}^{K'}$ on growth temperature throughout the modern day ocean. Significantly, the Atlantic and Pacific data sets exhibit no offset. The only offset observed is a small discrepancy between the high latitude North Atlantic and the Southern Ocean data sets.

4.2. Calibration of $U_{37}^{K'}$ With Alkenone Production Temperature

[15] The goal of calibration is to produce a robust, predictive equation which is unbiased over the range of parameter estimation [*Martens and Naes*, 1989]. No underlying functionality of the mathematical form of the calibration model is required or implied. The robustness of the calibration as an unbiased temperature estimator depends upon the degree to which the calibration data set represents the unknown population, i.e., its "representativity" [*Martens and Naes*, 1989]. The surface water alkenone calibration data (Table 1) includes samples collected over an extreme diversity of modern-day oceanic environments and provides maximum representativity of the calibration when applied to the paleo populations. Furthermore, non-temperature related factors that might influence alkenone

Table 3.   Alkenone Temperature Calibration Models[a]

Data Set	n	Temperature Range	Calibration Model	r^2	Standard Error of Estimate, °C
Surface Water Integrated Production Temperature (IPT)					
Atlantic region[b]	403	4–29°C	IPT = $48.673(U_{37}^{K'})^3 - 94.569(U_{37}^{K'})^2 + 80.716(U_{37}^{K'}) - 5.977$	0.97	1.1
Pacific	130	5–30°C	IPT = $24.676(U_{37}^{K'}) + 4.057$	0.97	1.3
Global[b]	567	−1–30°C	IPT = $28.321(U_{37}^{K'})^3 - 52.894(U_{37}^{K'})^2 + 54.293(U_{37}^{K'}) - 0.957$	0.97	1.2
Coretop Sediment Calibration With Mean Annual SST at 0 m Depth					
Global[c]	592	−1–29°C	AnnO = $29.876(U_{37}^{K'}) - 1.334$	0.97	1.1

[a] The number of data that are included in final calibration model (n) are the data remaining after outliers and data with excessive leverage were removed from the raw data sets (see text). Southern Ocean data from the Atlantic and Pacific sectors is not included in the regional calibrations.
[b] Anomalous SW Atlantic margin, NE Atlantic upwelling, and Nordic Sea data <4.0°C were excluded from calibration data. See text.
[c] Coretop samples from Nordic Sea and SW Atlantic margin were excluded from calibration data. See text.

unsaturation (e.g., light, nutrients) are represented in the calibration data and will contribute to the standard error of estimation.

[16] The primary assumption underlying a field calibration of $U_{37}^{K'}$ with surface water temperature is that the measured water temperature at the time of sampling approximates the average temperature of the alkenone production. This assumption is supported by observations that living algae rapidly adjust their alkenone unsaturation to changes in growth temperature [*Prahl et al.*, 1988, 2003; *Conte et al.*, 1998; *Epstein et al.*, 1998]. Furthermore, the turnover of particulate material in the surface mixed layer is generally short relative to the rate of change in mixed layer temperature and thus potential bias due to the presence of detrital alkenones synthesized at a different temperature should be minimal. However, as discussed below, this latter assumption may be invalid in regions where there are large gradients in alkenone production and/or temperature or rapid changes in temperature.

[17] We constructed alkenone production temperature calibrations for the regional Atlantic and Pacific data and for the combined global data (Table 3). We did not include the data sets from the southwest Atlantic margin, northeast Atlantic upwelling region and the Nordic Sea data from waters <4°C in the calibrations because these anomalous data have excessive leverage [*Neter and Wasserman*, 1974] and their inclusion in the calibration data set would greatly increase estimation error.

[18] To construct the calibration models, we first computed a third order polynomial regression of $U_{37}^{K'}$ versus temperature to identify and remove outliers and data with excessive leverage. For the Atlantic and global data sets, the higher order terms

were significant at the <0.05% level and thus were retained in the final model. For the Pacific data set, the higher order regression terms were not significant and so a linear calibration model was used.

[19] The mean standard error of temperature estimation is similar for the Atlantic and Pacific calibrations (1.1°C and 1.3°C, respectively, Table 3). The mean standard error of temperature estimation for the global calibration is 1.2°C, similar to the regional calibrations and indicative of the high degree of agreement among the Atlantic, Pacific and Southern Ocean data.

[20] Model residuals (measured – estimated temperature) exhibit a high degree of randomness and minimal trend across the entire range of temperature estimation (Figure 3). This indicates that the calibration models are generally unbiased estimators and can provide accurate estimates of production temperature across the range of ocean settings. Even so, a slight curvature in the Atlantic and global calibration residuals indicates that a polynomial model does not completely capture the nonlinear relationship between $U_{37}^{K'}$ and production temperature.

[21] In addition to the polynomial models, we also examined whether the use of logistic (or logit) transformed $U_{37}^{K'}$ data or a discontinuous model might improve the calibration for the temperate regions. The logit transformation, defined as

$$y' = \ln\left(\frac{y}{1-y}\right),$$

is useful for a dependent variable (i.e., $U_{37}^{K'}$) that has a curvilinear response function bounded by 0 and 1 because it often allows a simple linear regression model to be employed [*Neter and Wasserman*, 1974]. A major drawback of this type
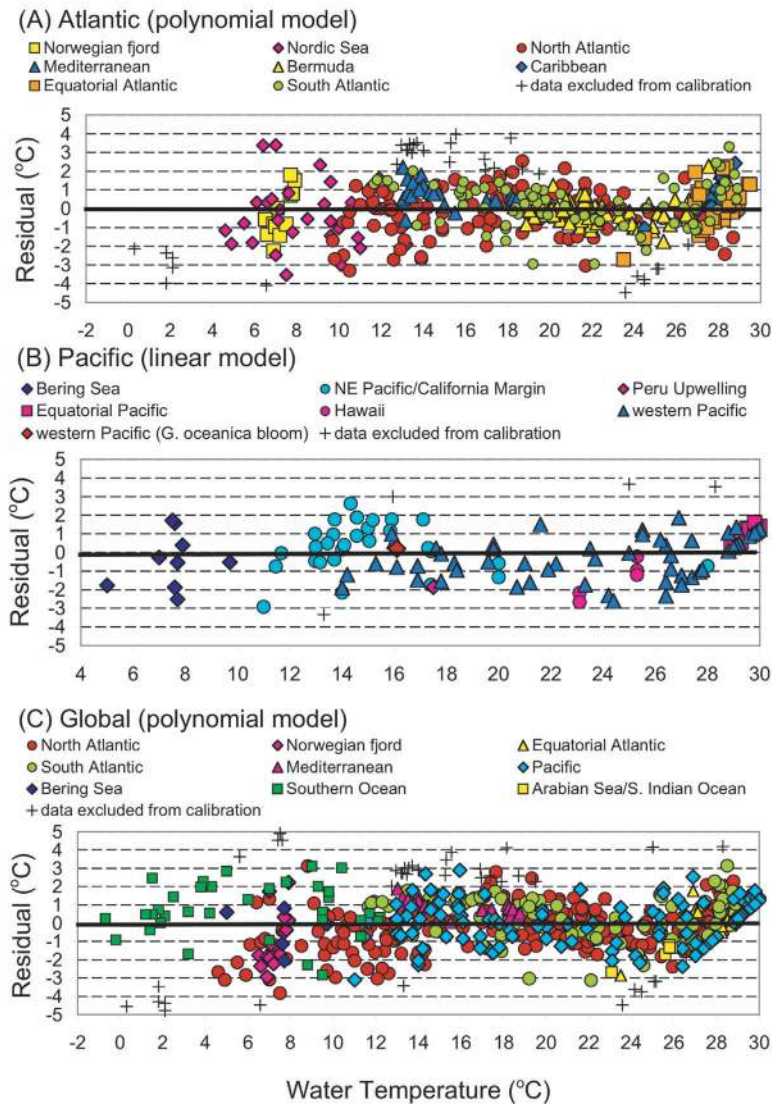
Figure 3. Residuals (measured - estimated temperature) of the surface water production temperature calibrations plotted against measured water temperature. The production temperature calibration models are given in Table 3. (a) Atlantic model. (b) Pacific model. (c) Global model. Samples that were excluded from the final calibration data set, including the anomalous samples from the western Argentine Basin (cf. Figure 2a), are indicated by crosses. Please note the Pacific regression does not include the Indian and Southern Ocean data.

of transformation is that it magnifies measurement errors near the asympototes of the function. We found that a logit model when applied only to the data subset collected between 10–25°C, or roughly in the middle range of the $U_{37}^{K'}$, did not improve the calibration relative to the polynomial model (data not shown). To evaluate the suitability of a discontinuous calibration model, we fit a linear regression to the data lying between 10–25°C, the most linear section of the response function (T = 5.6569 + 21.569($U_{37}^{K'}$), r^2 = 0.90). The residuals of this linear model exhibited strong curvature over

the calibration range (data not shown), and indicated that the response of alkenone unsaturation to growth temperature is in fact curvilinear throughout its range. Thus a linear calibration would result in systematic bias in estimated temperatures over the temperature range.

[22] To assess regional biases in estimated temperature when a global polynomial calibration model is universally employed, we compute the mean and standard deviation of residuals for each geographical region individually (Table 4). In all

Table 4. Mean and Standard Deviation of Model Residuals (Measured-Estimated Temperatures) for the Global Surface Water Production Temperature Calibration (Table 3) for Each Geographical Region

Geographic Region	Number of Data	Global Calibration	
		Mean	s.d.
Atlantic			
Norwegian fjord	13	−1.3	1.0
Nordic Sea	31	−1.1	1.6
North Atlantic	121	0.1	1.2
Mediterranean Sea	26	0.8	0.5
Bermuda	88	−0.1	0.7
Caribbean	20	0.4	0.8
Equatorial Atlantic (5°S–5°S)	35	0.1	1.1
South Atlantic	80	0.2	1.2
NE Atlantic low salinity	5	0.0	0.1
Pacific			
Bering Sea	12	1.3	2.4
Northeast Pacific	32	0.3	1.3
Hawaii	5	−0.9	1.0
Equatorial Pacific	12	1.2	0.4
Western Pacific	69	0.1	1.4
Peru Upwelling	1	−1.6	-
W. Pacific *G. oceanica* bloom	1	0.2	-
Indian/Arabian Sea	5	−1.7	0.6
Southern Ocean			
North of Antarctic polar front	24	0.9	1.6
South of Antarctic polar front	17	−0.3	1.4

regions except the small Arabian Sea data set, the residual mean is within two standard deviations of zero or less and indicates that regional bias in temperature estimation is insignificant (Table 4). Particularly significant is the absence of any bias in both the Atlantic and Pacific data sets despite their differences in alkenone-synthesizing populations and growth environments (Figures 2c and 3c). Overall, these results provide strong evidence that a single "global" calibration can be accurately used to estimate alkenone production temperature across the range of oceanic environments.

4.3. Influence of Lateral Advection on Surface Water Alkenone Distributions

[23] The Argentine Basin is a region of exceptionally strong surface currents and pronounced spatial gradients in productivity that result from the confluence of the cold northward flowing Malvinas Current and the warm southward flowing Brazil Current [*Gordon and Greengrove*, 1986; *Garzoli and Garraffo*, 1989; *Bianchi et al.*, 1993; *Provost et al.*, 1996]. The Malvinas current begins as an offshoot of the highly productive Antarctic Circumpolar Current [*Gordon and Greengrove*, 1986;

Provost et al., 1996]. As this strong current flows northward along the Argentine shelf/slope boundary, it is rapidly warmed by mixing and heat gain [*Gordon and Greengrove*, 1986; *Provost et al.*, 1996].

[24] *Benthien and Müller* [2000] previously reported that the alkenone $U^{K'}_{37}$ in coretop sediments in the Argentine Basin deviated significantly from that predicted by the *Müller et al.* [1998] global coretop AnnO calibration, and suggested that sedimentary alkenones in this region are affected by lateral sediment transport. The alkenone $U^{K'}_{37}$ in surface water samples from the western Argentine Basin similarly deviates from the global production temperature trend (Figures 2 and 3). Here we present evidence that this deviation results from rapid warming of the cold, highly productive Malvinas current as it flows northward toward the confluence region.

[25] In Figure 4a we map the measured water temperatures in surface water samples collected in the Argentine Basin. Also shown are the mean locations of the major current regimes in the area. The map shows that there is a large temperature gradient between samples collected in the core of the Malvinas current and the confluence region and samples collected in the surrounding waters.

[26] We computed the integrated production temperature (alkenone IPT) predicted by $U^{K'}_{37}$ in the surface water samples using the global production temperature calibration (Table 3). The alkenone IPT in the samples should be similar to the measured water temperature at the time of sample collection if the calibration model assumptions are valid within the region. However, within the core waters of the Malvinas Current and the confluence region with the Brazil Current, the alkenone IPT is lower than the measured temperature by as much as 2–3°C (Figure 4b). Significantly, the few samples collected in the Brazil-Malvinas confluence that do not show this temperature anomaly were collected on a previous year's cruise. In contrast, the temperature anomaly outside of this region is minimal except for a small cluster of data within a cold patch.

[27] The cold anomaly in alkenone $U^{K'}_{37}$ observed in the surface water of the Malvinas Current and confluence zone is consistent with northward advection of alkenones from cold, productive waters by the Malvinas Current and the rapid warming of this current as it flows toward the confluence zone. As living cells rapidly adjust alkenone unsaturation in response to changing temperature [*Prahl et al.*, 1988; *Conte et al.*, 1998], the apparent absence of any
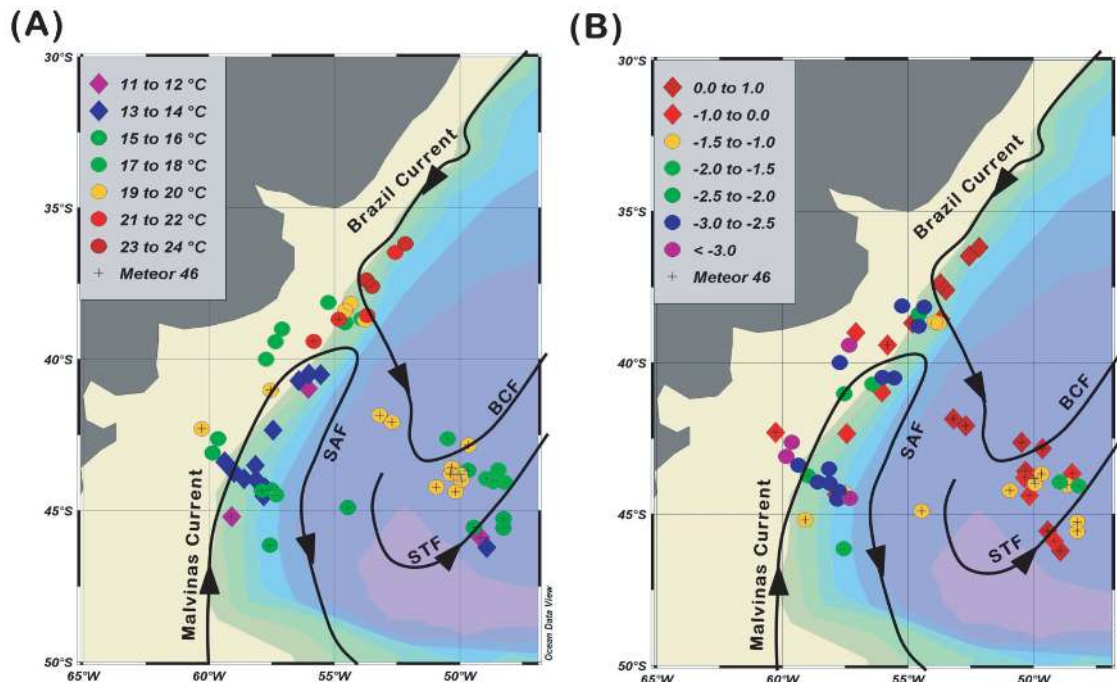
Figure 4. Alkenone and surface water temperature data from samples collected in the Brazil-Malvinas (Falkland) confluence region. Data were collected during austral summers of 2000 and 2001 on Meteor cruises M46/3 (hatched data) and M 49/2, respectively. The approximate locations of currents and fronts are redrawn from *Peterson and Stramma* [1991]. SAF, Subantarctic Front; STF, Subtropical Front; BCF, Brazil Current Front. (a) Measured water temperatures at the time of sample collection. (b) Difference between alkenone IPT and measured water temperature. Alkenone IPT was estimated using the global production calibration (Table 3).

significant compensatory adjustment in $U_{37}^{K'}$ as the waters warmed suggests a significant detrital component of "cold" alkenones in these samples relative to new compensatory alkenone production. This strong gradient in alkenone production is likely as nutrients within the surface waters of the Malivinas Current are rapidly depleted as it flows northward.

[28] In summary, intepretation of the alkenone temperature signal may be complex in sediments that underlie strong surface current systems and/or regions of extreme productivity and temperature gradients. In these settings, the alkenone signal may be significantly influenced by advection. The Argentine Basin analysis here further demonstrates that significant temperature anomalies can be generated even within the surface waters, so it is not necessary to invoke fine sediment transport [e.g., *Benthien and Müller*, 2000] exclusively.

4.4. Coretop Sediment Alkenone Distributions

[29] In Figure 5a we plot coretop $U_{37}^{K'}$ versus the overlying AnnO for the global sediment data set

(742 samples). As shown in Figure 1, these data are strongly weighted toward warmer regions and nearshore regions. We have updated the AnnO for each sample location using the revised Levitus 2001 surface temperature maps but otherwise have not edited the data sets. The coretop $U_{37}^{K'}$ versus AnnO for the different ocean regions generally agree except in the southwest Atlantic margin and the Nordic Sea, where there is evidence that the sedimentary alkenones have a large advected component [*Benthien and Müller*, 2000; *Bendle and Rosell-Melé*, 2004]. Because of this, we did not include either of these data sets in statistical analyses.

[30] The dependence of coretop $U_{37}^{K'}$ with overlying AnnO is best fit by a linear regression ($U_{37}^{K'}$ = 0.0709 + 0.0322T, n = 620, r² = 0.96). This updated regression is very similar to that originally published by *Prahl et al.* [1988] and recently updated by *Müller et al.* [1998] and *Müller and Fischer* [2003]. Even so, a slight flattening of the slope of coretop $U_{37}^{K'}$ versus overlying AnnO is apparent in Figure 5a at the temperature extremes (i.e., >25°C and <6°C), as is observed in surface water data.
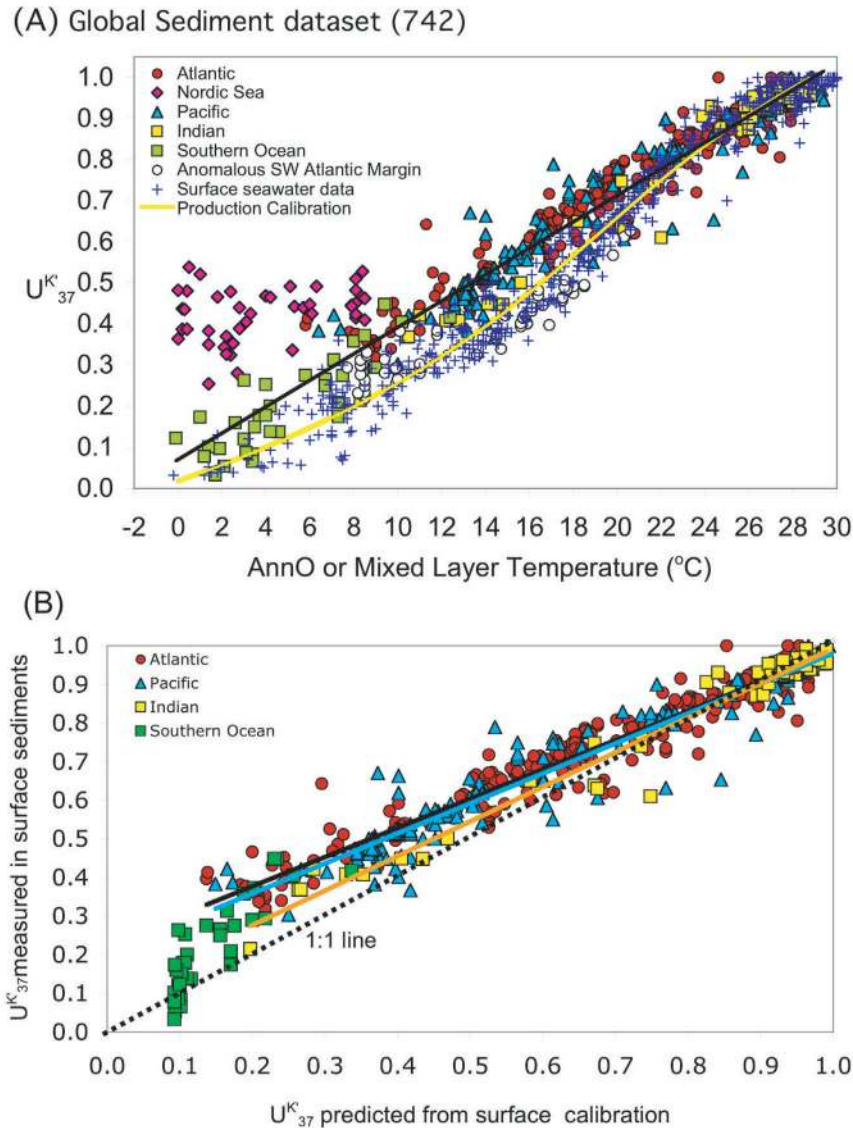
Figure 5. (a) $U_{37}^{K'}$ in coretop sediments plotted against overlying annual mean sea surface temperature at 0 m depth (AnnO). AnnO is estimated for each sample location using the updated Levitus et al. [2001] ocean temperature compilation [*Conkright*, 2002]. For comparison, the surface water $U_{37}^{K'}$ data (+) are also plotted against measured water temperature. The coretop AnnO calibration is shown by the solid black line. The surface water production temperature calibration is shown by the solid yellow line. (b) The $U_{37}^{K'}$ measured in surface sediments plotted against the $U_{37}^{K'}$ predicted in the sediments from the overlying AnnO. The predicted $U_{37}^{K'}$ is computed using the production temperature calibration (Table 3). The lines show linear fits to the Atlantic (black line), Pacific (blue line), and Indian (orange line) samples.

[31] We calibrate coretop $U_{37}^{K'}$ with overlying AnnO using the same procedure that was used for the surface water data. First, a third order polynomial regression was computed to remove outliers and data with excessive leverage. The regression was then recomputed. Because the higher order terms were not significant at the P < 0.05% level, they were not retained in the final coretop calibration model (Table 3). The standard error of AnnO estimation of the linear coretop calibration is 1.1°C, the same as that of the surface water production calibration.

[32] The residuals of the updated global coretop calibration for data from different regions are shown in Figure 6. There is a small positive bias in residuals for AnnO >25°C that reflects the slight curvature present in the data (cf. Figure 5a). The
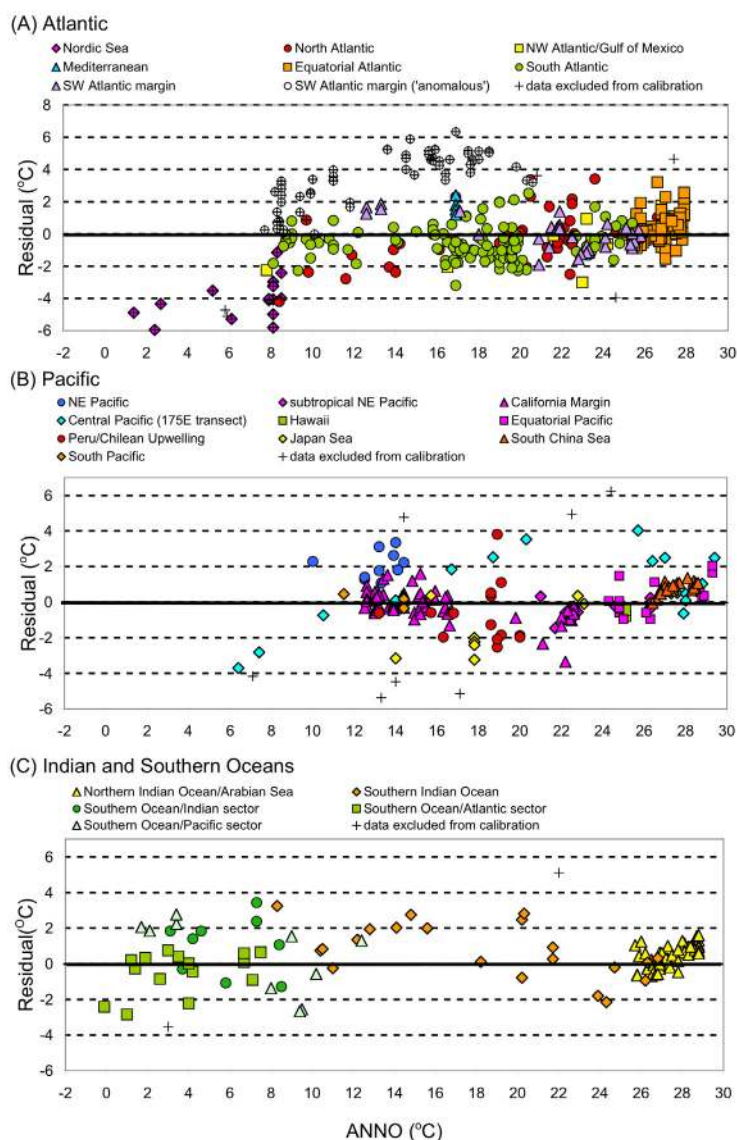
Figure 6. Residuals (measured - estimated temperature) of the sediment calibration plotted against AnnO. The AnnO calibration model is given in Table 3. (a) Atlantic data. (b) Pacific data. (c) Indian and Southern Ocean data. Offscale Nordic Sea data (i.e., samples with residuals less than −6°C) are not plotted.

residuals also exhibit somewhat higher regional offsets than observed for the surface waters (cf. Figure 3). For example, residuals from the North Atlantic and temperate southeast Atlantic are negatively biased whereas the Indian Ocean residuals are positively biased. For the northeast Pacific, the calibration closely fits the California margin data but samples collected farther offshore are positively biased. Significantly, the calibration poorly fits the central Pacific data, as evidenced by a strong trend in residuals for samples collected across the North Pacific front. These regional trends suggest that processes such as seasonality, coretop age, or advection influence the linkage between sediments

and the overlying surface waters differently in different regions.

4.5. Comparison of Alkenone Production Temperatures and Surface Sediment Distribution

[33] In Figure 5a, we have also plotted the surface water data on the same temperature scale, using the production temperature for surface water data. A high degree of overlap between these two data sets would be expected if the dependence of $U_{37}^{K'}$ on growth temperature has the same response function as the empirical correlation observed between core-

Table 5. ANOVA Regression Sums of Squares for the Full (SSE(F)) and Reduced (SSE(R)) Models and Calculations for Test of Equivalence of Surface Seawater and Sediment Regression Lines[a]

	Seawater (n1 = 590)		Sediment (n2 = 620)		Reduced Model (n = 1210)	
	SS	d.f.	SS	d.f.	SS	d.f.
Regression	47.532	3	30.089	3	78.577	3
Error	1.266	586	1.011	616	3.989	1206

[a] The regression model is $T = a + b\,(U_{37}^{K'}) + c\,(U_{37}^{K'})^2 + d\,(U_{37}^{K'})^3$, where T is the mixed layer temperature for surface seawater data and the annual mean SST (AnnO) for coretop sediment data. SSE(F) = 1.266 + 1.011 = 2.077. SSE(R) = 3.989. Calculation of F*:

$$F^* = \frac{(SSE(R) - SSE(F))}{((n1 + n2 - 4) - (n1 + n2 - 8))} \Big/ \frac{(SSE(F))}{(n1 + n2 - 8)} = \left(\frac{(3.989 - 2.077)}{4}\right) \Big/ \left(\frac{2.077}{1202}\right) = 276.63.\ F\ (0.999;\ 4;\ INF) = 4.62 \ll F^*.$$

top $U_{37}^{K'}$ and AnnO. However, the surface water and coretop data sets are clearly offset. In particular, the coretop $U_{37}^{K'}$ is consistently higher than the surface water $U_{37}^{K'}$ for temperatures <22°C.

[34] To statistically evaluate the difference between the surface water and coretop $U_{37}^{K'}$ versus temperature trends, we used a standard ANOVA test for the equivalence of two regression lines [*Neter and Wasserman*, 1974]. The test determines whether the error sum of squares in a reduced (i.e., combined surface water + sediment data) regression model is significantly less than the error sum of squares in the full (i.e., two separate regressions) model. We could use this test because the error terms for both regressions are normally distributed and have similar variances. The ANOVA sums of squares and calculations are shown in Table 5. The computed *F* statistic (F*) is highly significant at the ≪0.001 probability level, and confirms that the surface water and coretop regressions of $U_{37}^{K'}$ versus temperature are quite different.

[35] To better illustrate the offset between the sediment and surface water data, we used the global alkenone production temperature calibration (Table 3) to compute the $U_{37}^{K'}$ predicted in the coretop sediments if the sedimentary signal in fact does reflect the overlying AnnO. In Figure 5b we plot the predicted versus measured coretop $U_{37}^{K'}$ for each sediment sample (Figure 5c). The data significantly deviates from the 1:1 line. Interestingly, the observed slope of the deviation is <1, which indicates that the magnitude of the offset increases as $U_{37}^{K'}$ decreases (i.e., surface water temperatures decrease).

[36] It has been generally assumed that the coretop $U_{37}^{K'}$ integrates the mean temperature of alkenone production (the "integrated production temperature" or IPT), and that the coretop IPT approximates the present-day AnnO of overlying waters. However, the direct comparison shown in Figure 5 indicates that these assumptions do not appear to

be valid. One possibility is that because alkenone production is seasonal, the alkenone IPT in surface waters differs from the AnnO ("seasonality"). Several processes might also produce a spatial or temporal "mismatch" that decouples the coretop sediments from the overlying surface water environment. For example, as shown above lateral advection may affect the sedimentary alkenone inventory. Additionally, the sediments may be temporally decoupled due to decadal to century scales changes in upwelling intensity, current systems, frontal migration, etc. In areas of low sedimentation rates older alkenones may be mixed into surface sediments and contaminate the modern day signal. Finally, the initial $U_{37}^{K'}$ production ratio may have been altered in the water column and/or surficial sediments due to differential diagenesis of the di- and triunsaturated alkenones.

[37] The global calibration of $U_{37}^{K'}$ and production temperature derived here (Table 3) now allows us to independently compute the temperature that is recorded by $U_{37}^{K'}$ in the sediments (coretop IPT). We can thus explore the question: How closely does the coretop IPT match the overlying AnnO?

[38] We computed coretop IPT for the sediment $U_{37}^{K'}$ data using the global production temperature calibration and compared this with overlying AnnO. The difference between the coretop IPT and AnnO for sediment data from each ocean basin is plotted in Figure 7. Although various locations exhibit differences in the magnitude of the offset, coretop IPT is consistently warmer than AnnO for all sediments underlying surface waters where AnnO is approximately 22°C or less. Furthermore, the discrepancy between coretop IPT and AnnO increases as AnnO becomes colder.

[39] *Rosell-Melé et al.* [1995] first noted a "warm bias" in coretop alkenone temperatures in the eastern North Atlantic relative to overlying surface water production and hypothesized that this might
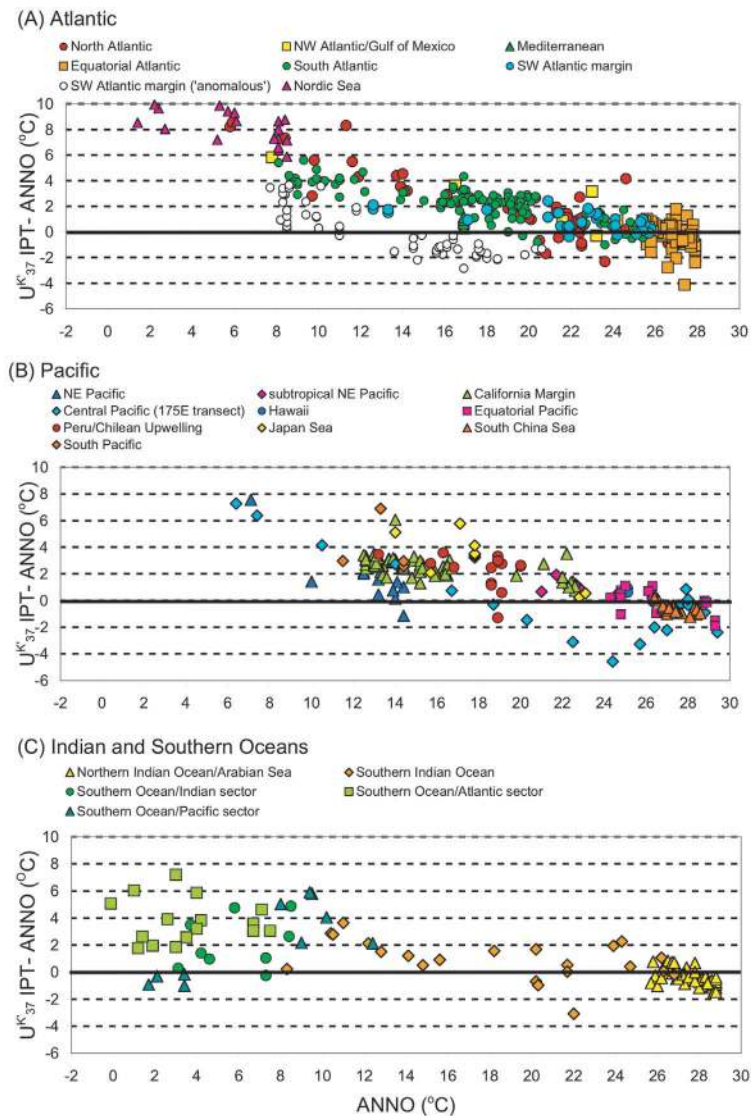
Figure 7. The difference between coretop IPT in sediments as recorded by $U_{37}^{K'}$ ($U_{37}^{K'}$IPT) and the overlying AnnO. Coretop IPT is calculated using the global production temperature calibration (Table 3). A positive deviation indicates that the coretop IPT estimate is warmer than AnnO. (a) Atlantic data. (b) Pacific data. (c) Southern Ocean and Indian Ocean data. Offscale Nordic Sea data are not plotted.

be due to faster degradation rates of more unsaturated alkenones (i.e., 37:4 > 37:3 >37:2). *Goñi et al.* [2001] also noted a "warm bias" in the sediment record in the Guaymas Basin relative to sediment trap flux. The greatly expanded sediment data set presented here indicates that this "warm bias" is generally universal.

4.6. Assessment of Causal Factors for the Offset Between Coretop IPT and AnnO

[40] The results above suggest that the surface water alkenone IPT does not equal to AnnO, the sedimentary signal is decoupled from the overlying

surface waters, and/or the coretop IPT has been altered post production. In this section, we examine these possibilities with the aid of simple models.

[41] A discrepancy between coretop IPT and overlying AnnO could arise if coretop IPT is not tightly coupled to the present-day surface water conditions. For example, the present-day frontal boundaries and intensities of upwelling regimes, which vary over annual to centennial time-scales, may not be representative of the interval integrated by the alkenones in the sediments. Additionally, in areas where sedimentation rates are low, coretop samples might also be contaminated with glacial material,

which would result in erroneously cold estimates of coretop IPT relative to the other sediment data. Both factors are very likely to affect the central North Pacific region, in particular. In other areas, fine particle advection might also bias in the sedimentary signal [e.g., *Thomsen et al.*, 1998; *Weaver et al.*, 1999; *Benthien and Müller*, 2000; *Rosell-Melé et al.*, 2000; *Ohkouchi et al.*, 2002; *Mollenhauer et al.*, 2005]. For example, there is a much smaller difference between coretop IPT and AnnO in the southwestern Atlantic margin sediments that have been influenced by advection from colder regions [*Benthien and Müller*, 2000] (Figure 7). Similarly, the northeast Pacific sediments offshore of the coastal upwelling region also exhibit a smaller offset, suggesting that they too might be influenced by advection from the colder and more productive upwelling area. However, although factors that spatially and temporally decouple the sediments from the present-day overlying surface water conditions are likely to introduce scatter and regional offsets among sediment data from different regions, it is difficult to envision how these processes could produce a universal and systematic offset of coretop IPT relative to AnnO.

[42] Seasonality and depth of production have also been cited as factors that might cause the alkenone temperature signal in sediments to deviate from AnnO (review by *Volkman* [2000]). Seasonality in alkenone production is very likely to create a systematic trend relative to AnnO because the alkenone production maximum shifts from winter/spring in low latitudes to summer in high latitudes. Seasonal variation in alkenone remineralization efficiency is also possible as alkenones are extensively remineralized during grazing [*Grice et al.*, 1998], and grazing pressure, in turn, is coupled to the seasonal production cycle.

[43] Latitudinal variations in thermocline production might also contribute to the observed trend with AnnO, although thermocline production alone could not be entirely responsible for the offset as this would generate a negative, not positive, offset of coretop IPT relative to AnnO. However, it could be hypothesized that the distinctive light and/or nutrient conditions and/or genotypes of alkenone synthesizers within the thermocline might alter the $U_{37}^{K'}$ temperature relationship, introducing bias in the coretop IPT estimate. For example, differences in the alkenone production temperature calibration have been observed in field populations under some conditions [*Conte et al.*, 1994, 2001; *Prahl et al.*, 2005]. However, this possibility seems

extremely unlikely for several reasons. First, the observed universality of the production temperature calibration strongly indicates that genetic and growth factors introduce minimal temperature bias. Secondly, the largest offset in the sediment data occurs in temperate and colder waters where alkenone production is largely confined to the mixed layer. Furthermore, even when a subsurface chlorophyll maximum is present, in situ ^{14}C alkenone production rates [*Hamanaka et al.*, 2000; *Shin et al.*, 2002; *Prahl et al.*, 2005] indicate that surface production predominates.

[44] We assess the potential influence of seasonality in production and/or remineralization efficiency on coretop IPT using a simple seasonality/remineralization model. We examined two hypothetical scenarios: (1) a midlatitude situation where alkenone production is maximum in early spring with smaller maximum in autumn (for example, that typical of the North Atlantic midlatitudes), and (2) a high latitude situation where production is confined to a strong maximum in summer (for example, that typical of the Southern Ocean). We assume alkenone remineralization to be constant or to vary as a function of primary production, to simulate a dependence of remineralization on grazing pressure [e.g., *Grice et al.*, 1998]. Alkenone remineralization was modeled as a linear, exponential or logarithmic function of production, with 10% of alkenones remineralized when production is at a minimum and 90% when production is at a maximum.

[45] The model results (Figure 8, Table 6) indicate that in the mid latitudes, seasonality in production under a constant remineralization efficiency results in only a small (~1°C) bias relative to AnnO. This offset is consistent with estimates of the seasonality bias in the field [*Ternois et al.*, 1996; *Sonzogni et al.*, 1997; *Müller et al.*, 1998; *Conte et al.*, 2001; *Müller and Fischer*, 2001, 2003]. Even in high latitude situation where production is confined to the summer period, the seasonality offset is only ~2.5°C. Covariation of remineralization efficiency with production would sharply reduce the magnitude of the offset.

[46] Alternatively, it has been suggested that remineralization efficiency might be reduced during periods of high productivity [*Berger et al.*, 1989; *Berger and Wefer*, 1990]. This would intensify the seasonality effect. Even under this scenario, the positive offset in coretop IPT relative to AnnO in all regions where AnnO is less than ~24°C would require that production is strongly skewed toward the summer months even in temperate and sub-
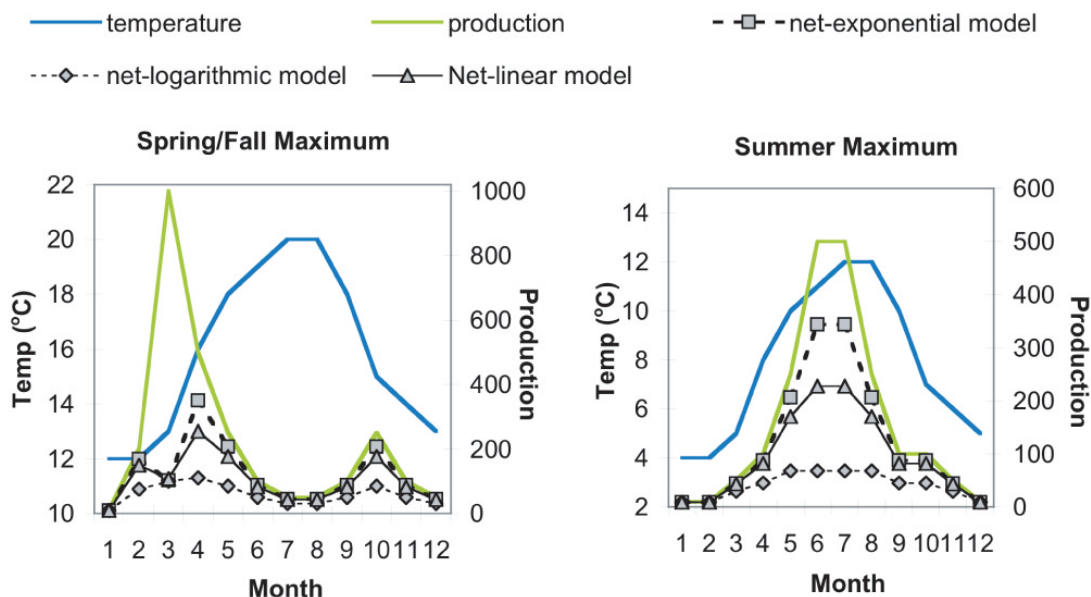
Figure 8. Hypothetical cases used to examine the effect of seasonality in alkenone production and/or water column remineralization on the annually averaged IPT of the alkenone flux. The graphs show the seasonal cycles in water temperature and alkenone production used in the model and the residual component of alkenone production under three variable remineralization models. The annually integrated alkenone IPT for the different models is given in Table 6.

tropical waters. This is not consistent with field studies of *E. huxleyi* and *Gephyrocapsa* spp. that find production is skewed toward colder temperatures at low and temperate latitudes [e.g., *Okada and McIntyre*, 1979; *Haidar and Thierstein*, 2001; *Brown and Yoder*, 1994; *Brown and Podestá*, 1997; *Cortés et al.*, 2001]. For example, alkenone IPT is approximately 1°C less than the AnnO in the

subtropical waters off Bermuda [*Conte et al.*, 2001]. Thus seasonality in production and/or remineralization efficiency by itself is unlikely to generate the positive offset observed.

[47] Finally, the positive offset between coretop IPT and AnnO in the global data set might result from diagenetic alteration of $U_{37}^{K'}$ in the water

Table 6. Effect of Seasonality in Alkenone Production and/or Remineralization on IPT of the Residual Fraction of the Alkenone Flux That Survives Degradative Losses[a]

		Residual Annually Integrated Alkenone IPT, °C			
	Annual Mean SST, °C	Model (1) Remineralization Constant	Model (2) Remineralization Exponential	Model (3) Remineralization Logarithmic	Model (4) Remineralization Linear
Case 1: mid latitude spring/fall production maximum	15.8	14.8	15.7	15.6	15.7
Case 2: high latitude summer production maximum	7.8	10.3	10.1	9.3	9.9

[a] Alkenone IPT is calculated using the global alkenone production temperature calibration (Table 3). The fraction of alkenones remineralized (FR) is modeled to remain constant or to vary as a function of total production, to simulate differential losses due to variable grazing pressure. For variable remineralization, an extreme case is examined where FR ranges from 0.1 at minimum production to 0.9 at maximum production. Four simple remineralization models are examined: (1) constant remineralization, FR(1) = 0.9; (2) remineralization varies exponentially with production, FR(2) = 0.0995e$^{0.022P}$; (3) remineralization varies logarithmically with production, FR(3) = 0.1737ln(P) − 0.3001; and (4) remineralization varies linearly with production, FR(4) = 0.0008P + 0.0919. The hypothetical production scenarios for Cases 1 and 2 and the residual alkenone production remaining under the three remineralization models are plotted in Figure 8.

column and/or in surficial sediments. Although most field studies have not detected any diagenetic alteration of $U_{37}^{K'}$ [e.g., *Prahl et al.*, 1993, 2001; *Conte et al.*, 1992; *Madureira et al.*, 1995; *Müller and Fischer*, 2001], *Hoefs et al.* [1998], and *Gong and Hollander* [1999] have presented equivocal evidence of differential degradation of the 37:3 and 37:2 alkenones in sediments, although these studies and their interpretation have been controversial [*Grimalt et al.*, 2000].

[48] We use a simple first order decay model to investigate the potential influence of differential degradation of 37:3 and 37:2 alkenones on the coretop IPT, with and without a seasonality offset. The decay model estimates the C37:3/C37:2 abundance ratio in the coretop sediments at time t, $\frac{[C37:2]_t}{[C37:3]_t}$, as

$$\frac{[C37:2]_t}{[C37:3]_t} = \frac{[C37:2]_0 e^{-at}}{[C37:3]_0 e^{-bt}} + \Delta S, \qquad (2)$$

where $\frac{[C37:2]_0}{[C37:3]_0}$ is the initial alkenone production ratio in the overlying surface waters, ΔS is the offset due to seasonality and/or thermocline production. The rate constants a and b are the degradation rate constants of the 37:2 and 37:3 alkenones, respectively.

[49] For a given AnnO, we calculate the coretop ratio $\frac{[C37:2]_t}{[C37:3]_t}$ using the empirical coretop AnnO calibration derived from the sediment data. Similarly, we calculate the initial alkenone ratio $\frac{[C37:2]_0}{[C37:3]_0}$ in the surface waters using the global production calibration (Table 3). If the alkenone IPT approximates AnnO (i.e., $\Delta S = 0$) and there has been no post-production alteration of $U_{37}^{K'}$ (i.e., the rate constants a and b are the same), the two ratios will be the same.

[50] The results for different values of AnnO are shown in Table 7. The observed difference between the initial production and coretop ratios indicates that $\Delta S \neq 0$ and/or the coretop ratio has been affected by diagenesis. We next explore these two possibilities.

[51] In Case #1, we assume a seasonality bias but no differential degradation. In this case, the magnitude of the seasonality offset ΔS is simply

$$\Delta S = \frac{[C37:2]_t}{[C37:3]_t} - \frac{[C37:2]_0}{[C37:3]_0}. \qquad (3)$$

The seasonality offset computed for Case #1 (Table 7) reflects the trendline of the offset observed in the sediment data (Figure 7) and is similar to that modeled (cf. Table 6). As noted above, the positive seasonality offset in all but tropical waters is not consistent with the seasonal production cycle of alkenone-synthesizing algae.

[52] In Case #2 we assume differential diagenesis but no seasonality ($\Delta S = 0$). Rearranging equation (2), and letting $X = \frac{[C37:2]_t}{[C37:3]_t}\frac{[C37:3]_0}{[C37:2]_0}$ the difference in the 37:3 and 37:2 rate constants is

$$\frac{\ln(X)}{t} = b - a \qquad (4)$$

[53] We assume a constant coretop age of 1000 years to calculate the differential degradation rate constant (b − a, Table 7). To explain the observed differences in the production and coretop ratios, these results indicate that in the absence of a seaonality effect, the differential degradation rate would need to vary as a function of AnnO. Alternatively, the coretop age would need to decrease as a function of AnnO when in fact, we would expect the opposite. There is no evidence for either trend, which suggests that differential degradation by itself is highly unlikely to generate the observed offset.

[54] In Case #3, we assume that both seasonality and diagenesis affect the coretop IPT. To estimate the approximate magnitude of the differential degradation rate, we have assumed that the surface water alkenone IPT equals AnnO at 21°C. We use this temperature as a first order estimate because it approximates the alkenone IPT off Bermuda [*Conte et al.*, 2001] and the maximum growth temperature for *E. huxleyi* and *G. oceanica* [*Brand*, 1982; *Conte et al.*, 1998]. For $\Delta S = 0$ at 21°C, the difference, b − a, is 1.99×10^{-4} (Case #2, Table 7). Assuming that the differential degradation rate is constant, we can calculate the magnitude of the seasonality offset using equation (4). The results (Case #3, Table 7) indicate a small positive seasonality bias in cold temperate and subpolar waters (AnnO < 15°C) and a slight negative bias in subtropical and tropical waters (i.e., >24°C). This result is consistent with field data that indicate a winter/spring (or upwelling) bias in alkenone production and a contribution from thermocline production at low latitudes, and a shift toward a summer bias in cold temperate and subpolar waters.

Table 7. Influence of Seasonality and/or Differential Alkenone Degradation on the Sedimentary Alkenone IPT Signal[a]

AnnO, °C	Sediment Ratio (Time t) 37:2/37:3	Production Ratio (Time 0) 37:2/37:3	Case 1 Seasonality Offset, No Differential Degradation Coretop IPT-AnnO (°C)	Case 2 Differential Degradation, No Seasonality Offset (for t = 1000 yrs) $b - a$ (x 10^{-4})	Case 3 Seasonality Offset and Differential Degradation (Annual IPT = AnnO @ 21 C) Sed IPT-AnnO (°C)
6	0.36	0.16	4.1	7.78	2.9
8	0.49	0.23	3.9	7.36	2.9
10	0.64	0.33	3.7	6.57	2.6
12	0.84	0.47	3.3	5.69	2.3
14	1.08	0.67	2.8	4.81	1.8
16	1.41	0.95	2.3	3.96	1.3
18	1.85	1.35	1.7	3.16	0.7
20	2.49	1.96	1.2	2.38	0.2
21	2.93	2.40	0.9	1.99	0.0
22	3.50	2.98	0.7	1.62	−0.2
23	4.26	3.76	0.4	1.25	−0.4
24	5.33	4.88	0.2	0.89	−0.5
26	9.70	9.43	−0.1	0.28	−0.6

[a] See text. Alkenone degradation is assumed to follow first order kinetics ($C37:2_t = C37:2_0 e^{-at}$ and $C37:3_t = C37:3_0 e^{-bt}$). Seasonality also includes the offset due to thermocline production. Alkenone production ratios in surface waters (time 0) and the residual in coretop sediments (time t) were estimated using the global production and coretop calibrations, respectively. The alkenone production ratio initially assumes that there is no seasonality or diagenesis effect. In Cases 1 and 2, the results show the seasonality offset or differential degradation rate that is required to generate the difference between the production and coretop ratios. In Case 3, the results show the seasonality offset for a constant differential degradation rate.

[55] The differential degradation rate that is required in this model to produce a seasonality bias that is consistent with field observations is small. Assuming a mean coretop age of 1000 years, the differential degradation rate we estimate is approximately 1.5 orders of magnitude less than the absolute degradation rates of 37:3 and 37:2 alkenones measured in abyssal North Atlantic sediments (mean 0.051 yr^{-1}, range 0.0096 to 0.1096 yr^{-1} [*Madureira*, 1994]).

[56] To summarize, the observed deviation between the coretop and surface water data can be reasonably explained if there is both a small bias in production IPT due to seasonality and/or thermocline production as well as a slight alteration in the coretop $U_{37}^{K'}$ from differential diagenesis in the water column and/or surficial sediments.

5. Conclusions

[57] Throughout ocean surface waters, a robust non-linear relationship exists between alkenone $U_{37}^{K'}$ and growth temperature. This relationship is statistically identical over the present-day diversity of open ocean environments and alkenone-synthesizing populations. The striking degree of agreement among the diversity of oceanographic settings indi-

cates that genetic and/or physiological factors that may affect alkenone unsaturation are small in the open ocean and exert only a minimal effect on the alkenone production temperature calibration.

[58] The global production temperature calibration we have derived here provides unbiased production temperature estimates over the entire range of modern ocean environments, with a mean standard error of estimated temperature is ±1.2°C. Regional bias in estimated temperature using the global calibration are insignificant, indicating that a single calibration can be universally applied for most paleoceanographic settings.

[59] The calibration of coretop $U_{37}^{K'}$ with overlying annual mean SST (AnnO), updated here using 742 data, is also robust with a mean standard error of estimated AnnO is ±1.1°C. There is somewhat higher regional bias than observed for surface water data, suggesting that processes affecting the coupling between sediments and overlying surface waters may introduce systematic biases under some circumstances.

[60] However, the linkage between alkenone production in surface waters and the temperature signal recorded by $U_{37}^{K'}$ in underlying sediments is not straightforward. The $U_{37}^{K'}$ in surface sediments

is systematically higher than predicted by the production temperature calibration in all but tropical waters. The magnitude of the offset increases as AnnO becomes colder. Simple model calculations indicate that seasonality and/or thermocline production alone are insufficient to generate the observed offset. However, the observed offset can be reasonably explained if differential diagenesis of C37:3 *versus* C37:2 in the water column and/or surficial sediments in addition to seasonality has influenced the sedimentary alkenone signal.

[61] This study also provides further evidence that the coupling between the coretop alkenone temperature signal and overlying surface waters can be significantly compromised by lateral advection in regions underlying strong currents where there are large temperature and productivity gradients.

Acknowledgments

References

Bac, M., K. R. Buck, F. P. Chavez, and S. C. Brassell (2003), Seasonal variation in alkenones, bulk suspended POM, plankton and temperature in Monterey Bay, California: Implications for carbon cycling and climate assessment, *Org. Geochem.*, *34*, 837–855.

Bendle, J., and A. Rosell-Melé (2004), Distributions of U_{37}^K and $U_{37}^{K'}$ in the surface waters and sediments of the Nordic Seas: Implications for paleoceanography, *Geochem. Geophys. Geosyst.*, *5*, Q11013, doi:10.1029/2004GC000741.

Bentaleb, I., J. O. Grimalt, F. Vidussi, J.-C. Marty, V. Martin, M. Denis, C. Hatté, and M. Fontugne (1999), The C_{37} alkenone record of seawater temperature during seasonal thermocline stratification, *Mar. Chem.*, *64*, 301–313.

Bentaleb, I., M. Fontugne, and L. Beaufort (2002), Long-chain alkenones and $U_{37}^{K'}$ variability along a south-north transect in the western Pacific Ocean, *Global Planet. Change*, *34*, 173–183.

Benthien, A., and P. J. Müller (2000), Anomalously low alkenone temperatures caused by lateral particle and sediment transport in the Malvinas Current region, western Argentine Basin, *Deep Sea Res., Part I*, *47*, 2369–2393.

Berger, W., and G. Wefer (1990), Export production: Seasonality and intermittancy and paleoceanographic implications, *Palaeogeogr. Palaeoclim. Palaeoecol.*, *89*, 245–254.

Berger, W. H., V. Smetacek, and G. Wefer (1989), Ocean productivity and paleoproductivity—An overview, in *Productivity of the Ocean—Present and Past*, edited by W. H. Berger, V. Smetacek, and G. Wefer, pp. 1–34, John Wiley, Hoboken, N. J.

Bianchi, A. A., C. F. Giulivi, and A. R. Piola (1993), Mixing in the Brazil-Malvinas Confluence, *Deep Sea Res., Part I*, *40*, 1345–1358.

Bijma, J., M. Altabet, M. Conte, H. Kinkel, G. J. M. Versteegh, J. K. Volkman, S. G. Wakeham, and P. P. Weaver (2001), Primary signal: Ecological and environmental factors—Report from Working Group 2, *Geochem. Geophys. Geosyst.*, *2*(1), doi:10.1029/2000GC000051.

Boon, J. J., F. w. Van der Meer, P. J. W. Schuyl, J. W. de Leeuw, P. A. Schenck, and A. L. Burlingame (Eds.) (1978), *Initial Reports of the Deep Sea Drilling Project, Vols. 38, 39, 40 and 41, Supplement, Walvis Ridge DSDP Leg 40*, pp. 627–637, U.S. Govt. Print. Off., Washington, D. C.

Brand, L. E. (1982), Genetic variability and spatial patterns of genetic differentiation in the reproductive rates of the marine coccolithophores *Emiliania huxleyi* and *Gephyrocapsa oceanica*, *Limnol. Oceanogr.*, *27*, 236–245.

Brassell, S. C., R. G. Brereton, G. Eglinton, J. Grimalt, G. Liebezeit, I. T. Marlowe, U. Pflaumann, and M. Sarnthein (1986), Palaeoclimatic signals recognized by chemometric treatment of molecular stratigraphic data, *Org. Geochem.*, *10*, 661–669.

Brown, C. W., and G. P. Podestá (1997), Remote sensing of coccolithophore blooms in the western South Atlantic Ocean, *Remote Sens. Environ.*, *60*, 83–91.

Brown, C. W., and J. A. Yoder (1994), Coccolithophore blooms in the global ocean, *J. Geophys. Res.*, *99*, 7467–7482.

Budziak, D. (2001), Late Quaternary monsoonal climate and related variations in paleoproductivity and alkenone derived sea-surface temperatures in the western Arabian Sea, *Ber. Fachber Geowiss. Univ. Bremen*, *170*, 1–114.

Cacho, I., C. Pelejero, and M. Canals (1999), C_{37} alkenone measurements of sea surface temperature in the Gulf of Lions (NW Mediterranean), *Org. Geochem.*, *30*, 557–566.

Chapman, M. R., N. J. Shackleton, M. Zhao, and G. Eglinton (1996), Faunal and alkenone reconstructions of subtropical North Atlantic surface hydrography and paleotemperature over the last 28 kyr, *Paleoceanography*, *11*(3), 343–358.

Conkright, M. E., et al. (2002), *World Ocean Database 2001*, vol. 1, *Introduction*, *NOAA Atlas NESDIS 42*, edited by S. Levitus, 167 pp., U.S. Govt. Print. Off., Washington, D. C.

Conte, M. H., and G. Eglinton (1993), Alkenone and alkenoate distributions within the euphotic zone of the eastern North Atlantic: Correlation with production temperature, *Deep Sea Res., Part I*, *40*, 1935–1961.

Conte, M. H., G. Eglinton, and L. A. S. Madueira (1992), Long-chain alkenones and alkyl alkenoates as paleotemperature indicators: Their production, flux and early sediment diagenesis in the eastern North Atlantic, in *Advances in Organic Geochemistry 1991*, edited by C. B. Eckardt and S. R. Larter, *Org. Geochem.*, *19*, 287–298.

Conte, M. H., A. Thompson, and G. Eglinton (1994), Primary production of lipid biomarker compounds by *Emiliania huxleyi*: Results from an experimental mesocosm study in Korsfjorden, southern Norway, *Sarsia*, *79*, 319–332.

Conte, M. H., A. Thompson, and G. Eglinton (1995), Lipid biomarker diversity in the coccolithophorid *Emiliania huxleyi* (Prymnesiophyceae) and the related species *Gephyrocapsa oceanica*, *J. Phycol.*, *31*, 272–282.

Conte, M. H., A. Thompson, D. Lesley, and R. P. Harris (1998), Genetic and physiological influences on the alkenone/alkenoate versus growth temperature relationship in *Emiliania huxleyi* and *Gephyrocapsa oceanica*, *Geochim. Cosmochim. Acta*, *62*, 51–68.

Conte, M. H., J. C. Weber, L. L. King, and S. G. Wakeham (2001), The alkenone temperature signal in western North Atlantic surface waters, *Geochim. Cosmochim. Acta*, *65*, 4275–4287.

Cortés, M. Y., J. Bollmann, and H. R. Thierstein (2001), Coccolithophore ecology at the HOT station ALOHA, Hawaii, *Deep Sea Res., Part II*, *48*, 1957–1981.

Doose, H., F. G. Prahl, and M. W. Lyle (1997), Biomarker temperature estimates for modern and last glacial surface waters of the California Current system betwen 33° and 42°N, *Paleoceanography*, *12*, 615–622.

Epstein, B. L., S. D'Hondt, J. G. Quinn, J. Zhang, and P. E. Hargraves (1998), An effect of dissolved nutrient concentrations on alkenone-based temperature estimates, *Paleoceanography*, *13*, 122–126.

Garzoli, S. L., and Z. Garraffo (1989), Transports, frontal motions and eddies at the Brazil-Malvinas Currents Confluence, *Deep Sea Res., Part A*, *36*, 70–681.

Gong, C., and D. J. Hollander (1999), Evidence for differential degradation of alkenones under contrasting bottom water oxygen conditions: Implication for paleotemperature reconstruction, *Geochim. Cosmochim. Acta*, *63*, 405–411.

Goñi, M. A., D. M. Hartz, R. C. Thunell, and E. Tappa (2001), Oceanographic considerations for the application of the alkenone-based paleotemperature $U_{37}^{K'}$ index in the Gulf of California, *Geochim. Cosmochim. Acta*, *65*, 545–557.

Gordon, A. L., and C. L. Greengrove (1986), Geostrophic circulation of the Brazil-Falkland Confluence, *Deep Sea Res., Part A*, *33*, 573–585.

Grice, K. W. C., M. K. Breteler, S. Schouten, and V. Grossi (1998), Effects of zooplankton herbivory on biomarker records, *Paleoceanography*, *13*, 686–693.

Grimalt, J. O., J. Rullkötter, M. Sicre, R. Summons, J. Farrington, H. R. Harvey, M. Goñi, and K. Sawada (2000), Modifications of the C_{37} alkenone and alkenoate composition in the water column and sediment: Possible implications for sea surface temperature estimates in paleoceanography, *Geochem. Geophys. Geosyst.*, *1*(11), doi:10.1029/2000GC000053.

Haidar, A. T., and H. R. Thierstein (2001), Coccolithophore dynamics off Bermuda (N. Atlantic), *Deep Sea Res., Part II*, *48*, 1925–1956.

Hamanaka, J., K. Sawada, and E. Tanoue (2000), Production rates of C_{37} alkenones determined by ^{13}C-labeling technique in the euphotic zone of Sagami Bay, Japan, *Org. Geochem.*, *31*, 1095–1102.

Harada, N., K. H. Shin, A. Murata, M. Uchida, and T. Nakatani (2003), Characteristics of alkenones synthesized by a bloom of *Emiliania huxleyi* in the Bering Sea, *Geochim. Cosmochim. Acta*, *67*, 1507–1519.

Herbert, T. D., J. D. Schuffert, and J.-C. Herguera (1998), Depth and seasonality of alkenone production along the California margin inferred from a core top transect, *Paleoceanography*, *13*, 263–271.

Hoefs, M. J. L., G. J. M. Versteegh, W. I. C. Rijpstra, J. W. de Leeuw, and J. S. S. Damsté (1998), Postdepositional oxic degradation of alkenones: Implications for the measurement of palaeo sea surface temperatures, *Paleoceanography*, *13*(1), 42–49.

Ikehara, M., K. Kawamura, and A. Taira (1997), Alkenone sea surface temperature in the Southern Ocean for the last two deglaciations, *Geophys. Res. Lett.*, *24*, 679–682.

Kennedy, J. A., and S. C. Brassell (1992), Molecular records of twentieth-century El Niño events in laminated sediments from the Santa Barbara basin, *Nature*, *357*, 62–64.

Kim, J.-H., R. R. Schneider, P. J. Müller, and G. Wefer (2002), Interhemisperic comparison of deglacial sea-surface temperature patterns in the Atlantic eastern boundary currents, *Earth Planet. Sci. Lett.*, *194*, 383–393.

Madureira, L. A. S. (1994), Lipids in recent sediments of the eastern North Atlantic, 287 pp., Ph.D. thesis, Univ. of Bristol, Bristol, UK.

Madureira, L. A. S., M. H. Conte, and G. Eglinton (1995), The early diagenesis of lipid biomarker compounds in North Atlantic sediments, *Paleoceanography*, *10*, 627–642.

Marlowe, I. T. (1984), Lipids as palaeoclimatic indicators, 273 pp., Ph.D thesis, Univ. of Bristol, Bristol, UK.

Marlowe, I. T., S. C. Brassell, G. Eglinton, and J. C. Green (1990), Long-chain alkenones and alkyl alkenoates and the fossil coccolith record of marine sediments, *Chem. Geol.*, *88*, 349–375.

Martens, H., and T. Naes (1989), *Multivariate Calibration*, 419 pp., John Wiley, Hoboken, N. J.

McCaffrey, M. A., J. W. Farrington, and D. J. Repeta (1990), The organic geochemistry of Peru margin surface sediments, 1, A comparison of the C_{37} alkenone and historical El Niño records, *Geochim. Cosmochim. Acta*, *54*, 1671–1682.

Mollenhauer, G., M. Kienast, F. Lamy, H. Meggers, R. R. Schneider, J. M. Hayes, and T. I. Eglinton (2005), An evaluation of ^{14}C age relationships between co-occurring foraminifera, alkenones, and total organic carbon in continental margin sediments, *Paleoceanography*, *20*, PA1016, doi:10.1029/2004PA001103.

Müller, P. J., and G. Fischer (2001), A 4-year sediment trap record of alkenones from the filamentous upwelling region off Cape Blanc, NW Africa and a comparison with distributions in underlying sediments, *Deep Sea Res., Part 1*, *48*, 1877–1903.

Müller, P. J., and G. Fischer (2003), C_{37} alkenones as paleotemperature tool: Fundamentals based on sediment traps and surface sediments from the South Atlantic Ocean, in *The South Atlantic in the Late Quaternary: Reconstruction of Material Budget and Current Systems*, edited by G. Wefer, S. Mulitza, and V. Ratmeyer, pp. 169–195, Springer, New York.

Müller, P. J., G. Kirst, G. Ruhland, I. von Storch, and A. Rosell-Melé (1998), Calibration of the alkenone paleotemperature index $U_{37}^{K'}$ based on core-tops from the eastern South Atlantic and the global ocean (60°N–60°S), *Geochim. Cosmochim. Acta*, *62*, 722–1757.

Neter, J., and W. Wasserman (1974), *Applied Linear Statistical Models*, 842 pp., Irwin-Dorsey, Georgetown, Ontario, Canada.

Ohkouchi, N., K. Kawamura, and H. Okada (1999), Depth ranges of alkenone production in the central Pacific Ocean, *Global Biogeochem. Cycles*, *13*, 695–704.

Ohkouchi, N., T. L. Eglinton, L. D. Keigwin, and J. M. Hayes (2002), Spatial and temporal offsets between proxy records in a sediment drift, *Science*, *298*, 1224–1227.

Okada, H., and A. McIntyre (1979), Seasonal distribution of modern coccolithophores in the western North Atlantic Ocean, *Mar. Biol.*, *54*, 319–328.

Pelejero, C., and E. Calvo (2003), The upper end of the $U_{37}^{K'}$ temperature calibration revisited, *Geochem. Geophys. Geosyst.*, *4*(2), 1014, doi:10.1029/2002GC000431.

Pelejero, C., and J. O. Grimalt (1997), The correlation between the $U_{37}^{K'}$ index and sea surface temperatures in the warm boundary: The South China Sea, *Geochim. Cosmochim. Acta*, *61*, 4789–4797.

Peterson, R. G., and L. Stramma (1991), Upper-level circulation in the South Atlantic Ocean, *Prog. Oceanogr.*, *26*, 1–73.

Prahl, F. G., and S. G. Wakeham (1987), Calibration of unsaturation patterns in long-chain ketone compositions for palaeotemperature assessment, *Nature*, *330*, 367–369.

Prahl, F. G., L. A. Muehlhausen, and D. L. Zahnle (1988), Further evaluation of long-chain alkenones as indicators of paleoceanographic conditions, *Geochim. Cosmochim. Acta*, *52*, 2303–2310.

Prahl, F. G., L. A. Muehlhausen, and M. Lyle (1989), An organic geochemical assessment of oceanic conditions at MANOP site C over the past 26,000 years, *Paleoceanography*, *4*, 495–510.

Prahl, F. G., R. B. Collier, J. Dymond, M. Lyle, and M. A. Sparrow (1993), A biomarker perspective on prymnesiophyte productivity in the northeast Pacifc Ocean, *Deep Sea Res., Part I*, *40*, 2061–2076.

Prahl, F. G., C. H. Pilskaln, and M. A. Sparrow (2001), Seasonal record for alkenone in sedimentary particles from the Gulf of Maine, *Deep Sea Res., Part I*, *48*, 515–528.

Prahl, F. G., M. A. Sparrow, and G. V. Wolfe (2003), Physiological impacts on alkenone paleothermometry, *Paleoceanography*, *18*(2), 1025, doi:10.1029/2002PA000803.

Prahl, F. G., B. N. Popp, D. M. Karl, and M. A. Sparrow (2005), Ecology and biogeochemistry of alkenone production at Station ALOHA, *Deep Sea Res., Part I*, *52*, 699–719.

Provost, C., V. Garcon, and L. M. Falcon (1996), Hydrographic conditions in the surface layers over the slope-open ocean transition area near the brazil-Malvinas Confluence during austral summer 1990, *Cont. Shelf Res.*, *16*, 215–235.

Rosell-Melé, A. (1998), Interhemispheric apprasial value of alkenone indices as temperature and salinity proxies in high latitude locations, *Paleoceanography*, *13*, 694–703.

Rosell-Melé, A., G. Eglinton, U. Pflaumann, and M. Sarnthein (1995), Atlantic core-top calibration of the $U_{37}^{K'}$ index as a sea-surface paleotemperature indicator, *Geochim. Cosmochim. Acta.*, *59*, 3099–3107.

Rosell-Melé, A., P. Comes, P. J. Miller, and P. Ziveri (2000), Alkenone fluxes and anomalous $U_{37}^{K'}$ values during 1989–1990 in the northeast Atlantic (48°N 21°W), *Mar. Chem.*, *71*, 251–264.

Sawada, K., N. Handa, Y. Shiraiwa, A. Danbara, and S. Montani (1996), Long-chain alkenones and alkyl alkenoates in the coastal and pelagic sediments of the northwest North Pacific, with special reference to the reconstruction of *Emiliania huxleyi* and *Gephyrocapsa oceanica* ratios, *Org. Geochem.*, *24*, 751–764.

Sawada, K., N. Handa, and T. Nakatsuda (1998), Production and transport of long-chain alkenone and alkyl alkenoates in a sea water column in the northwestern Pacific off central Japan, *Mar. Chem.*, *59*, 219–234.

Shin, K.-H., N. Tanaka, N. Harada, and J.-C. Marty (2002), Production and turnover rates of C_{37} alkenones in the eastern Bering Sea: Implication for the mechanism of a long duration of *Emiliani huxleyi* bloom, *Prog. Oceanogr.*, *55*, 113–129.

Sicre, M., E. Bard, U. Ezat, and F. Rostek (2002), Alkenone distributions in the North Atlantic and Nordic sea surface waters, *Geochem. Geophys. Geosyst.*, *3*(2), 1013, doi:10.1029/2001GC000159.

Sikes, E. L., and L. D. Keigwin (1994), Equatorial Atlantic sea surface temperature for the last 30 kyr: A comparison of $U_{37}^{K'}$, $\delta^{18}O$ and foraminiferal assemblage temperature estimates, *Paleoceanography*, *9*, 31–45.

Sikes, E. L., and J. K. Volkman (1993), Calibration of alkenone unsaturation ratios ($U_{37}^{K'}$) for paleotemperature estimation in cold polar waters, *Geochim. Cosmochim. Acta*, *57*, 1883–1889.

Sikes, E. L., J. W. Farrington, and L. D. Keigwin (1991), Use of the alkenone unsaturation ratio $U_{37}^{K'}$ to determine past sea surface temperatures: Core top SST calibrations and methodology considerations, *Earth Planet. Sci. Lett.*, *104*, 36–47.

Sikes, E. L., J. K. Volkman, L. G. Robertson, and J.-J. Pichon (1997), Alkenones and alkenes in surface waters and sediments of the Southern Ocean: Implications for paleotemperature estimation in polar regions, *Geochim. Cosmochim. Acta*, *61*, 1495–1505.

Sonzogni, C., E. Bard, and G. Eglinton (1997), Core-top calibration of the alkenone index vs. sea surface temperature in the Indian Ocean, *Deep Sea Res., Part II*, *44*, 1445–1460.

Ternois, Y., M.-A. Sicre, A. Boireau, J.-C. Marty, and J.-C. Miquel (1996), Production pattern of alkenones in the Mediterranean Sea, *Geophys. Res. Lett.*, *23*, 3171–3174.

Ternois, Y., M.-A. Sicre, A. Boireau, M. H. Conte, and G. Eglinton (1997), Evaluation of long-chain alkenones as paleo-temperature indicators in the Mediterranean Sea, *Deep Sea Res., Part I*, *44*, 271–286.

Thomsen, C., D. E. Schulz-Bull, G. Petrick, and J. C. Duinker (1998), Seasonal variability of the long-chain alkenone flux and the effect on the $U_{37}^{K'}$ index in the Norwegian Sea, *Org. Geochem.*, *28*, 311–323.

Volkman, J. K. (2000), Ecological and environmental factors affecting alkenone distributions in seawater and sediments, *Geochem. Geophys. Geosyst.*, *1*(9), doi:10.1029/2000GC000061.

Volkman, J. K., G. Eglinton, E. D. S. Corner, and J. R. Sargent (1980), Novel unsaturated straight-chain C_{37}–C_{39} methyl and ethyl alkenones in marine sediments and a coccolithophore *Emiliania huxleyi*, in *Advances in Organic Geochemistry 1979*, edited by A. G. Douglas and J. R. Maxwell, pp. 219–227, Elsevier, New York.

Volkman, J. K., S. M. Barrett, S. I. Blackburn, and E. L. Sikes (1995), Alkenones in *Gephyrocapsa oceanica*: Implications for studies of paleoclimate, *Geochim. Cosmochim. Acta*, *59*, 513–520.

Weaver, P. P. E., M. R. Chapman, G. Eglinton, M. Zhao, D. Rutledge, and G. Read (1999), Combined coccolith, formanifera, and biomarker reconstruction of paleoceanographic conditions over the last 120 kyr in the northern North Atlantic (59°N–23°W), *Paleoceanography*, *14*, 336–349.

Yamamoto, M., Y. Shiraiwa, and I. Inouye (2000), Physiological responses of lipids in *Emiliania huxleyi* and *Gephyrocapsa oceanica* (Haptophyceae) to growth status and their implications for alkenone paleothermometry, *Org. Geochem.*, *31*, 799–811.